

TRIGGERS FOR THE DETECTION OF GRAVITATIONAL WAVE BURSTS

N. ARNAUD, F. CAVALIER, M. DAVIER, P. HELLO AND T. PRADIER

Laboratoire de l'Accélérateur Linéaire

B.P. 34

Bâtiment 208, Campus d'Orsay

91898 Orsay Cedex, France

We present several filtering methods which can be used as triggers for the detection of gravitational wave bursts in interferometric detectors. All the methods are compared to matched filtering with the help of a *figure of merit* based on the detection of supernovae signals simulated by Zwerger and Müller.

1 Introduction

Supernovae have been historically the first envisaged source of gravitational waves (GW). Although binary inspirals or even periodic GW emitters like pulsars seem to be nowadays more promising sources, impulsive sources of GW such as supernovae should also be considered in the data analysis design of interferometric detectors currently under construction.

Impulsive GW sources are typically collapses of massive stars, leading to the birth of a neutron star (type II supernova)^{1,2,3} or of a black hole⁴; mergers of compact binaries can also be considered as impulsive sources⁵.

The problem with these sources is that the emitted waveforms are very poorly predicted, unlike the binary inspirals. As a consequence, this forbids the use of matched filtering for the detection of GW bursts in the data of one interferometric detector. The filtering of such bursts should therefore be as general and robust as possible and with minimal *a priori* assumptions on the waveforms to be detected: A drawback is of course that such filters will be sensitive to non-stationary noises as well as to GW bursts; spurious events, e.g. generated by these transient noises, should be eliminated afterwards when working in coincidence with other detectors. But, on the other hand, burst filters could help to identify and understand these noises, which would be useful especially during the debugging phase of the detector.

We present in the following some filtering methods dedicated to the detection of GW bursts: methods based on the autocorrelation, slope detector, correlator ... All the filters are compared by studying their performance to detect a reference sample of GW burst signals; for this purpose, just as in⁶ (and in order to use somewhat physically sound signals), we use the catalogue of signals emitted by type II supernovae, numerically computed by Zwerger and Müller (ZM)² and available on the web⁷.

Throughout the following, we assume that the detector noise is white, stationary and Gaussian with zero mean. For the numerical estimates, we chose the flat (amplitude) spectral density to be $h_n \simeq 4 \times 10^{-23} / \sqrt{\text{Hz}}$ and the sampling frequency $f_s \simeq 20 \text{ kHz}$, so the standard deviation of the noise is $\sigma_n = h_n \sqrt{f_s/2} \sim 3 \times 10^{-21}$; we will note the sampling time $t_s = 1/f_s$. The value

chosen for h_n corresponds approximately to the minimum of the sensitivity curve of the VIRGO detector⁸; around this minimum, the sensitivity is rather flat, in the range $\sim [200 \text{ Hz}, 1\text{kHz}]$, which is precisely the range of interest for the gravitational wave bursts we are interested in. This validates then our assumption of a white noise; otherwise, we can always assume that the detector output has been first whitened by a suitable filter⁹.

2 General filters

2.1 Filters based on the autocorrelation

The noise being whitened, its autocorrelation is ideally a Dirac function, and, in practice vanishes outside of 0. The autocorrelation of the data $x(t)$

$$A_x(\tau) = \int x(t)x(t+\tau)dt \quad (1)$$

should then reveal the presence of some signal (surely correlated). The information contained in the autocorrelation function can be extracted in different ways. We have studied two of them and built so two non-linear filters. The first one computes the maximum of the autocorrelation $A_x(\tau)$; this occurs always at $\tau = 0$, and then this maximum is nothing but the norm of $x(t)$. For sampled data x_i in a window of size N , the output of this filter is simply

$$A(0) = \sum_{i=1}^N x_i^2. \quad (2)$$

In the following, we will refer to this filter as the Norm Filter (NF). A similar approach has been developed independently by Flanagan and Hughes in the context of the detection of binary black hole mergers¹⁰.

Another simple possibility is to look at the norm of the autocorrelation function :

$$||A|| = \sqrt{\frac{1}{N} \sum_{k=2}^N A(k)^2}, \quad (3)$$

where $A(k)$ denotes the discrete autocorrelation of N data x_i . The sum is here initiated at the second bin according to the fact that the noise (uncorrelated) contributes essentially to the first bin. In the following we will call this filter Norm of Autocorrelation (NA). In practice, the $A(k)$ are computed in the Fourier space, according to the Wiener-Khintchine theorem, allowing the use of FFT's. Note that the only parameter for these two filters is the window size N .

2.2 The Bin Counting filter

This filter (BC) computes the number of bins in a window of size N whose value exceeds some threshold $s \times \sigma_n$. For example, if we take $s = 2$ and pure Gaussian noise, as $P(|x_i| \geq 2\sigma_n) \simeq 4.6\%$, the output of the BC filter is on average about 46 'counts' for a window size $N = 1000$. This filter is also non-linear, but it involves two parameters : the window size N and the threshold s . The threshold s is chosen by maximizing the signal to noise ratio (SNR) when detecting the signals of the ZM catalogue. The optimum is for $s \simeq 1.7$ but it is not critical; indeed any value of s in the range $[1.4, 2.0]$ would be also convenient (with a low loss in SNR).

2.3 The Slope Detector

This filter (SD) fits the data in a window of size N to a straight line. If the data are pure white noise with zero mean, then the slope of the fitted line is zero on average, so this slope detector

can well discriminate between the two cases : only noise or noise+signal. The output of the SD is simply

$$a = \frac{\langle tx \rangle - \langle t \rangle \langle x \rangle}{\langle t^2 \rangle - \langle t \rangle^2} = \frac{1}{N} \sum_{i=1}^N \frac{t_i - \langle t \rangle}{\langle t^2 \rangle - \langle t \rangle^2} x_i, \quad (4)$$

where $\langle y \rangle = \sum_{i=1}^N y_i / N$ denotes the mean value of the y_i and $t_i = i \times t_s$. Note that this filter is linear, as opposed to the first three considered. Again the only parameter is the window size N .

2.4 The Peak Correlator

Filtering by correlating the data with peak (or pulse) templates is justified by the fact that simulated supernova GW signals exhibit one (or more) peaks. The pulse templates have been built from truncated Gaussian functions

$$F_\tau(t) = \exp\left(-\frac{t^2}{2\tau}\right), \quad (5)$$

with $-3\tau \leq t \leq 3\tau$. The only parameter of the peak correlator (PC) is the width of the Gaussian pulse filter τ (the window size is automatically set to be a power of 2, due to use of FFT's). The lattice of filters is then built as usual (see¹¹ for example) : the distance $\Delta\tau$ between two successive filters of the lattice F_τ and $F_{\tau+\Delta\tau}$ is computed by the condition

$$\frac{\langle F_\tau, F_\tau \rangle - \langle F_{\tau+\Delta\tau}, F_\tau \rangle}{\langle F_\tau, F_\tau \rangle} \leq \epsilon, \quad (6)$$

where we define a scalar product as $\langle f, g \rangle = \text{Max}_t \int f(t+t')g(t)dt / \sqrt{\int f^2(t)dt}$ and ϵ is the allowed loss in the SNR. A simple calculation leads to $\Delta\tau = 2\tau\sqrt{\epsilon}$. With $\epsilon = 10^{-2}$, we finally have 26 templates in the interval [0.1 ms, 10 ms] (which are used in the following).

2.5 Statistics

The SD and PC filters being linear, they transform an input normal Gaussian noise with zero mean into a Gaussian noise with zero mean but with a modified standard deviation. For the SD filter, with the help of Eq.4, we find a standard deviation

$$\sigma_{\text{SD}}^2 = \sum_{i=1}^N \left(\frac{t_i - \langle t \rangle}{N(\langle t^2 \rangle - \langle t \rangle^2)} \right)^2 = \frac{12f_s^2}{N(N^2 - 1)}. \quad (7)$$

Similarly, when correlating pure noise data with the pulse filter F_τ , we obtain a Gaussian noise of standard deviation

$$\sigma_{\text{PC}}^2 = \sqrt{\pi} \frac{\tau}{t_s}. \quad (8)$$

The output of the BC filter is a binomial random variable, considering the data are pure Gaussian random variables; it is well approximated by Gaussian statistics for long enough windows (typically $N \geq 50$)¹² and the standard deviation for the noise at the BC output is simply

$$\sigma_{\text{BC}} = \sqrt{Np(1-p)} \quad (9)$$

with $p = \text{erfc}(s/\sqrt{2})$.

Considering the NF filter, if we call A its output, it is easy to see that A follows a chi-square distribution with N degrees of freedom, and then $A^* = \sqrt{2A} - \sqrt{2N-1}$ is also well approximated by a normal ($\sigma_{\text{NA}} = 1$) Gaussian random variable, provided $N \geq 30$ ¹², and the input noise is itself a normal Gaussian random variable.

Finally, the noise at the output of the NA filter is not known analytically and its characteristics have to be found numerically (adding some complexity to this filtering method).

3 Performance of the filters

3.1 Definition of a threshold for detection

We set the false alarm rate for each of the filters to be 10^{-6} (72 false alarms / hour for a sampling rate $f_s = 20$ kHz). This corresponds to a detection threshold (normalised SNR) of $\eta \simeq 4.89$ for a single 'Gaussian filter'. For a trigger that incorporate in fact several filters, for example the 26 templates of the PC, the threshold has to be raised accordingly, in order to keep a global false alarm rate of 10^{-6} (e.g. $\eta \simeq 5.50$ in this case).

3.2 The Zwerger and Müller Catalogue

The catalogue of Zwerger and Müller⁷ (ZMC) contains 78 gravitational-wave signals. Each of them corresponds to a particular set of parameters, essentially the initial distribution of angular momentum and the rotational energy of the star core, in the axisymmetric collapse models of ZM. The signal total durations range from about 40 ms to a little more than 200 ms. The gravitational wave amplitudes of the stronger signals are of the order $h \sim$ a few 10^{-23} for a source located at 10 Mpc. All the signals are computed for a source located at 10 Mpc. We can then re-scale the waveforms in order to locate the source at any distance d , according to

$$h(d, t) = h_0(t) \frac{10\text{Mpc}}{d} \quad (10)$$

where h_0 is the signal at 10 Mpc and $h(d, t)$ is the same signal but at a distance d . Concerning the shape of the waveforms, Zwerger and Müller distinguish three different types of signals⁴. Type I signals typically present a first peak (associated to the bounce) followed by a ringdown. Type II signals show a few (2-3) decreasing peaks, with a time lag between the first two of at least 10 ms. Type III signals exhibit no strong peak but fast (~ 1 kHz) oscillations after the bounce.

Since the 78 signal waveforms are known, we can explicitly derive the optimal SNR provided by the Wiener filter matched to each of them, and then compute the maximal distance of detection. We will then be able to build a benchmark for the different filters by comparing their results (detection distances) to the results of the Wiener filter. Note that, in what follows, we consider optimally polarized GW's, along the interferometer arms.

Let's call $h(t)$ one of the 78 signals (at some distance d) and $\tilde{h}(f)$ its Fourier transform. The optimal signal to noise ratio ρ_0 is given by

$$\rho_0^2 = 2 \int \frac{|\tilde{h}(f)|^2}{S_h(f)} df = \frac{f_s}{\sigma_n^2} \int |\tilde{h}(f)|^2 df = \frac{f_s}{\sigma_n^2} \int |h(t)|^2 dt, \quad (11)$$

where $S_h = h_n^2$ is the one-sided noise power spectral density (hence the factor of 2).

As previously, a supernova signal is detected by the Wiener filter if $\rho_0 \geq \eta$, where η is the same detection threshold as defined above. Fig.1 shows the maximal distance of detection for each of the 78 signals. The mean distance, averaged over all the signals, is about $\bar{d}_{\text{opt}} \simeq 25.4$ kpc, which is of the order of the diameter of the Milky Way. A few signals can be detected at distances beyond 50 kpc, the distance of the Large Magellanic Cloud (LMC). It is clear that this class of signals will be detected by the first generation interferometric detectors only if the supernovae occur inside our Galaxy or in the very close neighbourhood.

3.3 Estimating a filter performance

Let's consider one signal, say the i^{th} in the ZMC. The optimal filtering allows to detect such a signal for a source located at the distance $d_i^{(0)}$. Similarly, a filter F is able to detect the same

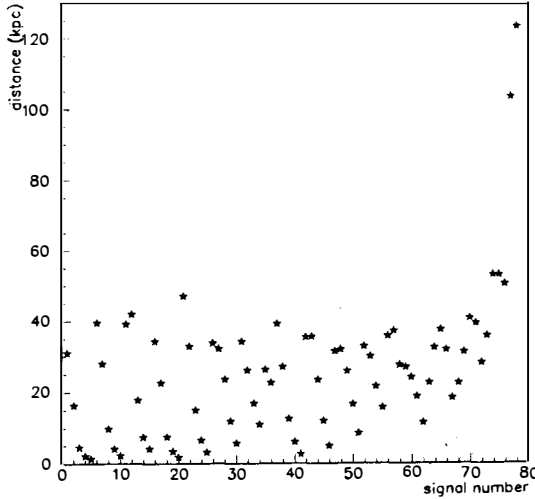


Figure 1: Detection distances calculated with the optimal filter for the 78 signals in the ZMC

signal up to a distance d_i ; of course d_i is averaged over many noise realizations in a Monte Carlo simulation. The detection efficiency of the filter F for this signal i is simply defined as the distance of detection relative to the optimal distance of detection : $d_i/d_i^{(0)}$. The global performance of the filter F is then estimated as the detection efficiency averaged over all the signals of the ZMC :

$$\rho = \frac{1}{78} \sum_{i=1}^{78} \frac{d_i}{d_i^{(0)}}. \quad (12)$$

3.4 Comparison of the filtering methods

The results for the different filters are reported in the Table 1 below. We also give the average distance of detection $\bar{d} = \frac{1}{78} \sum_{i=1}^{78} d_i^{(i)}$ for all the filters, together with the ratio $\bar{d}/\bar{d}_{\text{opt}}$.

Table 1: Efficiency of the different filters. L means linear filter and NL means non-linear filter.

Filter	Optimal	NF	NA	BC	SF	PC
d (kpc)	25.4	11.5	11.4	10.9	20.7	18.5
$\bar{d}/\bar{d}_{\text{opt}}$	1	0.45	0.45	0.43	0.81	0.73
ρ	1	0.46	0.47	0.43	0.79	0.73
Linearity	L	NL	NL	NL	L	L

The three first filters NF, NA and BC (all non-linear) have an efficiency a little less than one half, while the SD and the PC have an efficiency a little above 0.7. note that the SF has been in fact implemented with a sampling of 6 different window sizes, sufficient to cover the variety of signals. If implemented with a single window size, as the other filters NF, NA and BC, its performance decreases down to about 0.6.

4 Conclusion

We have discussed several filters to be used as triggers for detecting GW bursts in interferometric detectors. They are all sub-optimal but their efficiency is not far below that of optimal filter.

Concerning the detection of ZMC like signals, we note that none of the BC, NF and NA filters is efficient enough to cover the whole Galaxy in average, at the contrary of the SD and PC (and optimal) filters. Several signals can be 'seen' in fact anywhere from the Galaxy and even beyond; in particular the signals 77 and 78 can be detected up to the LMC by any of the filters.

Finally, all the filters studied here can be implemented on line without problem, due to use of FFT's (for the NA and the PC) or to simple recurrence relations between filter outputs in successive windows (NF,BC or SD).

More information (preprints, Virgo reports ...) can be found at¹³

References

1. S. Bonazzola and J.-A. Marck, *Astron. Astrophys.* **267**, 623 (1993).
2. T. Zwerger and E. Müller, *Astron. Astrophys.* **320**, 209 (1997).
3. M. Rampp, E. Müller and M. Ruffert, *Astron. Astrophys.* **332**, 969 (1998).
4. R.F. Stark and T. Piran, *Phys. Rev. Lett.* **55**, 891 (1985).
5. M. Ruffert and H.-Th. Janka, *Astron. Astrophys.* **338**, 535 (1998).
6. N. Arnaud, F. Cavalier, M. Davier and P. Hello, *Phys. Rev. D* **59**, 082002 (1999).
7. <http://www.mpa-garching.mpg.de/~ewald/GRAV/grav.html>
8. The "official" VIRGO sensitivity curve is available at :
<http://www.pg.infn.it/virgo/presentation.htm>
9. M. Beccaria, E. Cuoco and G. Curci, "Adaptive Identification of VIRGO-like noise spectrum", internal VIRGO report VIR-NOT-PIS-1390-096 (1997).
10. E.E. Flanagan and S.A Hughes, *Phys. Rev. D* **57**, 4535 (1998).
11. B.S. Sathyaprakash and S.V. Dhurandhar, *Phys. Rev. D* **44**, 3819 (1991).
12. M.R. Spiegel, "Probabilités et statistique, Cours et problèmes" (McGraw-Hill, Paris, 1981).
13. <http://www.lal.in2p3.fr/virgo/DAD/dadweb.html>